Physicochem. Probl. Miner. Process., 60(3), 2024, 189217

http://www.journalssystem.com/ppmp

Physicochemical Problems of Mineral Processing

ISSN 1643-1049

Leaching behaviour of limonite ores from Lapaopao, Southeast Sulawesi, Indonesia: Effect of mineralogy and acid types

Suharto Onggang [1], Adi Maulana [1,2], Sufriadin [3], Ulva Ria Irfan [1,2]

[1] Earth and Environmental Technology Study Program, Faculty of Engineering, Hasanuddin University, Makassar, Indonesia

[2] Geological Engineering Department, Faculty of Engineering, Hasanuddin University, Makassar, Indonesia

[3] Mining Engineering Department, Faculty of Engineering, Hasanuddin University, Makassar, Indonesia

Corresponding author: sufri.as@unhas.ac.id (Sufriadin)

Abstract: An atmospheric leaching study of limonite ores from Lapaopao, Southeast Sulawesi, using hydrochloric acid (HCl), nitric acid (HNO_3), and sulfuric acid (H_2SO_4) has been performed. The objectives of this study were to analyze the effect of ore mineralogy and acid types on the dissolution behavior of minerals and the leaching rate of Ni and Co at atmospheric pressure conditions. Mineralogical analysis was carried out using optical microscopy, scanning electron microscopy (SEM), and X-ray diffractometry (XRD), while the ore's chemical composition was determined by using X-ray fluorescence spectrometry (XRF) and atomic absorption spectrophotometry (AAS). Mineralogically, the limonite ores are dominated by goethite, followed by gibbsite, talc, and lizardite, with less amounts of hematite and quartz. Analysis results of solid residues revealed that mineral dissolution order was determined as follows: goethite > lizardite > gibbsite> hematite > talc> quartz. The results of the leaching experiment exhibited that the order of leaching rates of Ni in the three ores samples using three different acids were found as follows: Ore-1 > Ore-2 > Ore-3. Comparison of HCl, HNO_3, and H_2SO_4 as the lixiviants for the leaching of limonite ores demonstrated that HCl was the most reactive acid, followed by HNO_3 and then H_2SO_4. This might be due to the differences in mineralogical nature and reactivities of acids during the leaching process.

Keywords: limonite ore, atmospheric leaching, hydrochloric acid, nitric acid, sulfuric acid

1. Introduction

Today, nickel is one of the critical metals that has become a very attractive commodity and has increased demand over the coming decades due to the intensive development of electric vehicles, where nickel is an important element for battery manufacturing (International Energy Agency, 2022; International Nickel Study Group, 2021; Whitworth et al., 2022). Nickel is produced from two distinct ore types: nickel sulfide and nickel laterite deposits. Approximately 73% of the world's nickel resources come from laterite deposits and only about 23% from sulfide deposits (Butt, 2007; Dalvi et al., 2004). Nickel laterite deposits are formed through the laterization of ultramafic rocks resulting from the supergene and enrichment processes (Marsh et al., 2013). In the laterization process of ultramafic rocks, the following layers are included: 1) the limonite layer (upper layer, containing < 1.5% Ni, and it is hosted in iron minerals such as goethite and hematite); 2) the saprolite layer (middle layer, containing > 1.5% Ni, and it is hosted in serpentine, talc, or smectite); and 3) ultramafic bedrocks (lower zone, containing <0.4% Ni, and it is mainly held in olivine). Nickel is highly concentrated and enriched in limonite and saprolite layers (Dalvi et al., 2004; Golightly, 1979).

Two options are currently employed in the processing of Ni laterite ores: the pyrometallurgical and hydrometallurgical routes. The pyrometallurgical method is applied to treat the lateritic nickel ore to produce Fe-Ni, Ni matte, or NPI by smelting the ores in an electric furnace (Kyle, 2010). However, this technology can only economically process moderate- to high-grade nickel ore or saprolite (>1.5% Ni) due to the high energy requirement of the process. The hydrometallurgical method is applied for the

DOI: 10.37190/ppmp/189217

processing of lower-grade ores or limonite (<1.5% Ni) by acid leaching (Agatzini-Leonardou et al., 2009; Kyle, 2010). The advantages of this technology are low temperature operation and the fact that, in addition to Ni-Co, some other valuable elements can be recovered simultaneously (Teitler et al., 2022). Further two hydrometallurgical methods that are recently applied, namely pressure acid leaching (PAL) and atmospheric leaching (AL). However, due to the precipitation of iron as hematite during the leaching process, the conventional sulfuric acid pressure leaching (PAL) procedure had been the preferred method for the extraction of Ni and Co from laterites (mainly limonite). Higher capital and operational costs, more acid neutralization, and issues with PAL's commercial-level construction were the main downsides of the PAL process. As a result, leaching at atmospheric pressure (AL) has drawn increasing attention in recent years (Li et al., 2012). The drawbacks of sulfuric acid atmospheric leaching are longer leaching times and higher acid consumption (Stanković et al., 2020). However, the AL method also offers several advantages and future prospects, such as lower investment costs, lower energy consumption, simpler process equipment, faster ramp-up periods, and easier maintenance with high on-stream availability (Önal and Topkaya, 2014).

Other two leaching reagents, in addition to sulfuric acid, have been intensively employed for the extraction of Ni and Co from laterite ores, namely nitric acid and chloride acid. Despite the fact that no commercial stage has been developed by using those reagents, nitric acid has the following advantages (He et al.,2022). (a) The leaching reactions are mild, with low temperature and pressure; (b) It is easy to be regenerated and recycled, leading to the low reagent consumption; (c) The residue does not contain sulfur, implying the potential utilization of iron and chromium. Similarly, chloride acid has some advantages over sulfuric acid, including better solubility of complex ores, better stability of chloride complexes, and regeneration of extraction reagents. In addition, its dissolution ability increases dissolution kinetics and thus reduces equipment size and operating temperatures, and extends the range of operating conditions (Garces-Granda et al., 2020).

Despite a lot of leaching studies performed to recover Ni and Co from limonite ores using these acids, the utilization of such acids in the experimental leaching process at a time is rarely done. It is suspected that limonite ores with different characteristics of mineralogy and elemental compositions would have different dissolution behaviors and thereby different extraction rate of metals during the leaching process. A better understanding about mineralogical properties, including the texture and chemistry of limonite ores, is important in elucidating the leaching mechanism of limonite ores in various acid solutions (Wang et al., 2012). Therefore, the objectives of this paper were to discuss the dissolution behavior of minerals and compare the extraction rates of Ni-Co from Lapaopao limonite ores using HCl, HNO_3, and H_2SO_4 at atmospheric pressure.

2. Materials and methods

2.1. Materials

Three limonite ore samples were collected from the Lapaopao mine area that are considered representative, having various mineral and chemical composition. Such samples are denoted to Ore-1, Ore-2, and Ore-3 respectively. Lapaopao area is located in Kolaka Regency, Southeast Sulawesi Province, Indonesia. The map showing the sample location area is illustrated in Fig. 1. The limonite ore was taken for approximately 25 kg of each sample for this study.

2.2. Methods

This study was conducted in three stages: 1) field work, 2) laboratory work, and 3) data analysis and interpretation (Fig. 2). Field work was carried out for collecting the limonite ore samples and gathering all the data and information required in the field. Laboratory work includes sample preparation, sample characterization, and leaching experiments. The limonite ore samples were sent to a laboratory, where they were air-dried for several days to remove their surface moisture. Samples were homogenized and then reduced in particle size using a jaw crusher and ball mill before being submitted for analysis and a leaching experiment. For optical microscopic observation, about 5 grams of raw ore samples were embedded with epoxy resin and then polished to ensure surface flatness. Meanwhile, for XRD analysis, samples were ground using agate mortar to produce powder materials.

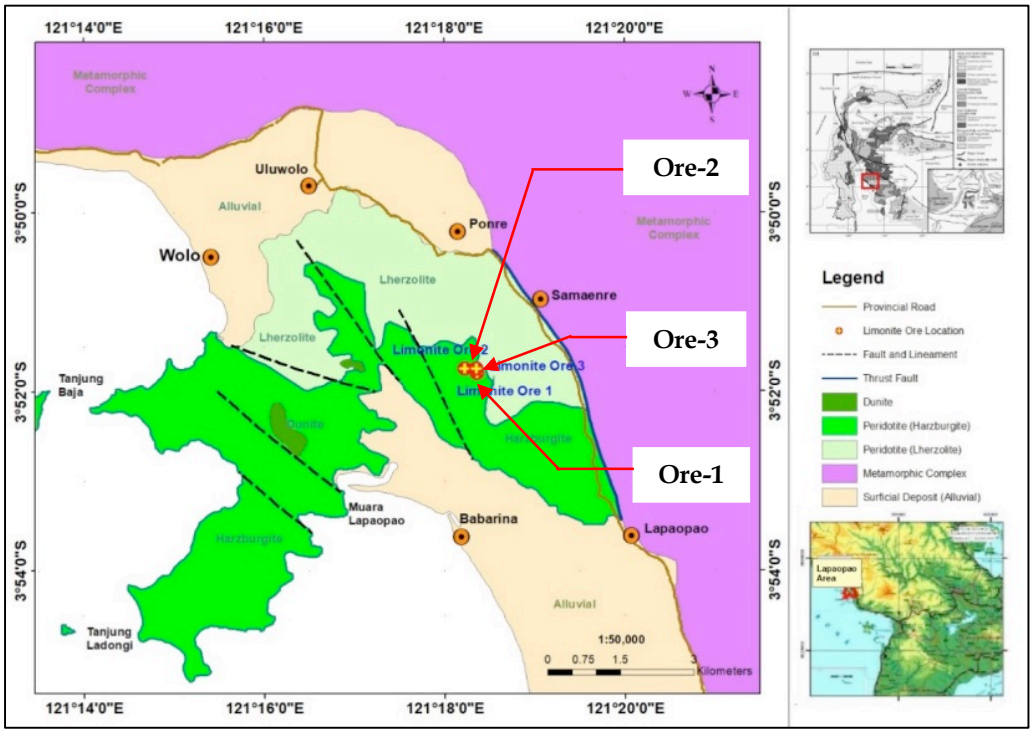

Fig. 1. Geological map of Lapaopao and sample location (Modified from Parawangsa et al., 2021)

The ore texture and mineralogical characteristics of limonite ore samples were examined by using a polarizing light microscope (Nikon Eclipse LV100N POL) under the polished section, XRD (Shimadzu Maxima X-7000 diffractometer), and SEM-EDX (Quanta FEI-450). For the XRD analysis, the sample was scanned at room temperature using Cu-Kα radiation with a voltage of 40 kV and a current of 30 mA. The scan range (2θ angle) was 5-70◦ with a step size of 0.02°. All these analyses were carried out at the Department of Geological Engineering, Hasanuddin University. The chemical composition of limonite ore samples was determined using the XRF method (Bruker S8 Tiger WDXRF spectrometer) at Sucofindo Samaenre Laboratory and an atomic absorption spectrometer (AAS) at Sucofindo Laboratory, Makassar, respectively.

A batch atmospheric leaching experiment of three different limonite ore samples was conducted using a 2-necked flask with a 500 mL capacity. A digital hot plate magnetic stirrer (Corning PC-420D model) was utilized for heating the flask. A reflux condenser was attached to the reactor to prevent evaporation. A thermometer was attached to the flask to monitor the temperature during leaching. HCl, HNO_3, and H_2SO_4 with respective concentrations of 4 M were used as leaching reagents. The experimental conditions were set as follows: particle size of <75 µm, temperature of 100 °C, solid-to-liquid ratio of 1:7, and stirring speed of 450 rpm. After the leaching experiment was completed, the pregnant leach solutions (PLS) and leach residues were separated using a filter membrane with a diameter of 0.45 microns. The PLS were further analyzed by AAS to determine Ni and Co content. Leach residues were washed with deionized water three times to remove their acid content and then were dried in oven with the temperature of 100 ◦C for two hours. After that, solid residues were examined by using XRD and SEM to find out the phases and morphological changes, respectively. These works were done at the Mineral Processing Laboratory, Department of Mining Engineering, Hasanuddin University, Makassar.

3. Results and discussion

3.1. Limonite ore characterization

3.1.1. Ore mineralogy

The results of microscopic and SEM analyses of ore samples are provided in Fig. 3. It is shown that limonite or e samples were dominated by goethite, followed by gibbsite. Goethite is characterized by

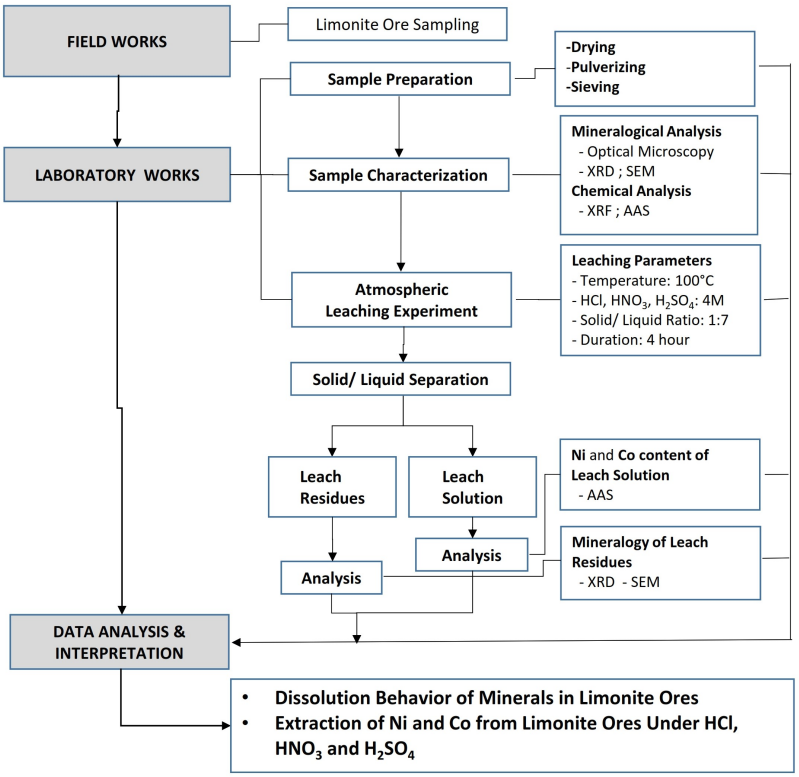

Fig. 2. The flowchart showing the research stages and leaching experiment of this study

an acicular texture. Talc, lizardite, and maghemite or hematite were also detected within the samples. The presence of maghemite or hematite is indicated by being bright and isotropic. Goethite and gibbsite show moderate reflectivity, while talc, lizardite, and quartz demonstrate low reflectivity. Most minerals likely have subrounded to irregular shapes with a wide range in grain sizes. It can be interpreted that Ni and Co are most likely held in goethite structures (Carvalho-e-Silva et al., 2003; Cornell and Schwertmann, 2006; Gharaei et al., 2019) and possibly in gibbsite (Putzolu et al., 2018) and lizardite as well (Pelletier, 1996).

The X-ray diffraction patterns of the three limonite ore samples used in this study are depicted in Fig. 4. The presence of diffraction peaks with d-spacings around 4.15 Å, 2.43 Å, and 1.71 Å are characteristics of goethite. Gibbsite was detected by the occurrence of peaks with basal spacings of about 7.83 Å, 2.69 Å, and 2.23 Å. The reflection intensities occurring with d values of 9.26 Å, 3.11 Å, and 1.56 Å are diagnostic peaks of talc. Lizardite, a serpentine group, was recognized in Ore-2 by the occurrence of reflection intensity at 12.16° 2θ (7.26 Å). Quartz was identified by the presence of a peak at 26.63° 2θ corresponding to a d-spacings of 3.34 Å.

Table 1. Semi quantitative XRD analysis of minerals containing in the three limonite ore samples from Lapaopao, Southeast Sulawesi

Mineral	Formula	Ore-1 (%)	Ore-2 (%)	Ore-3 (%)	Average (%)
Goethite	FeO(OH)	54.0	36.6	36.8	42.47
Gibbsite	Al $(OH)_3$	25.5	11.9	20.2	19.20
Talc	$Mg_3(Si_4O_{10})(OH)_2$	10.0	8.1	25.9	14.67
Lizardite	$Mg_3(Si_2O_5)(OH)_4$	2.6	33.6	nd	12.07
Hematite	α-Fe_2O_3	nd*	3.3	14.8	6.03
Maghemite	γ-Fe_2O_3	1.1	nd	nd	0.37
Quartz	SiO_2	6.8	6.6	2.4	5.27

*nd=not detected

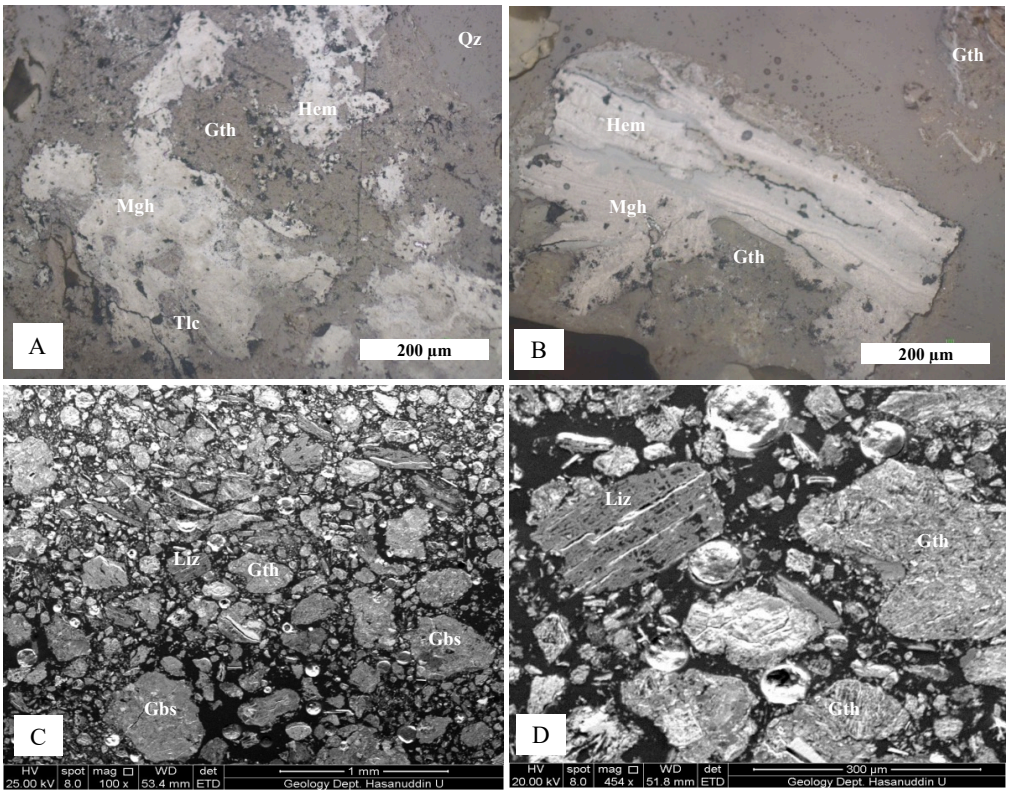

Fig. 3. Optical photomicrographs (A and B) and backscattered electron (BSE) images (C and D) of limonite ore samples from Lapaopao showing various textures. Gth goethite, Gbs gibbsite, Tlc talc, Mgh maghemite, Hem hematite, and Qz quartz. The mineral abbreviation names follow Whitney and Evans, (2010)

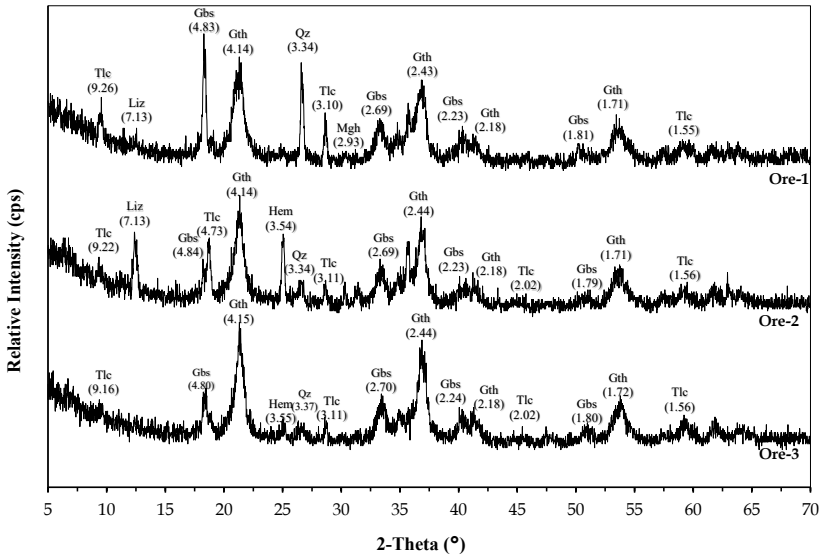

Fig. 4 XRD patterns of the three of Limonite samples e.g. Ore-1, Ore-2, and Ore-3 from Lapaopao. Gth = Goethite, Gbs= Gibbsite, Mgh= Maghemite, Tlc= Talc, Hem= Hematite, Liz= Lizardite, and Qz= Quartz. Note: unit of d-spacing is angstrom (Å)

The semi-quantitative mineralogy of the three limonite ore samples was estimated using Impact Match! 3 software (Table 1). Results show that goethite, gibbsite, and talc constitute almost 90% of the minerals in Ore-1. The rest of the minerals consist of lizardite, quartz, and maghemite. There are relatively similar proportions of goethite and lizardite in Ore-2, with amounts up to 70%. Other phases such as gibbsite, talc, hematite, and quartz comprise about 30%. In Ore-3, goethite was still dominant,

followed by talc and gibbsite. Significant quantities of hematite were found in Ore-3 with values of almost 15%, whereas quartz was estimated to have less than 3%. Lizardite and hematite were not detected in Ore-3.

3.1.2. Ore chemistry

The results of the chemical analysis of three limonite ore samples from Lapaopao as determined by XRF are shown in Table 2. All samples are predominantly composed of Fe_2O_3 (>56%). This is consistent with the dominance of goethite as the main iron-bearing mineral in the samples. Hematite could also be the source of Fe_2O_3. The elevated concentrations of Al_2O_3 (>10%) can be attributed to the presence of gibbsite in the samples. Nonetheless, Al could also be incorporated into the goethite structure. Silica (SiO_2) has a wide concentration range between 4.14% and 14.02%. The presence of SiO_2 is not only supplied by quartz but also by talc and lizardite. Magnesia (MgO) shows lower grades, with values ranging from 1.23% to 2.30%. Similarly, the content of other major oxides, such as TiO_2 and MnO, is low as well. The concentration of Ni is highest in Ore-2, followed by Ore-1, and the lowest grade is in Ore-3. In contrast, the Cr_2O_3 grade is highest in Ore-3, and the lowest content is in Ore-1. Cobalt shows very low values for all samples (<0.1). Based on the chemical composition of the three samples as shown in Table 2, these samples are best categorized as limonite ores.

Table 2. The chemical composition of the limonite ores from Lapaopao as determined by XRF analysis

Oxides/Elements	Composition (%)		
	Ore-1	Ore-2	Ore-3
SiO_2	14.02	11.75	4.14
Al_2O_3	11.35	13.02	15.52
TiO_2	0.25	0.23	0.29
Fe_2O_3	56.28	56.19	60.03
MgO	1.34	2.30	1.23
MnO	0.55	0.61	1.30
Cr_2O_3	2.27	2.94	3.34
LOI (Loss on Ignition)	13.00	12.30	14.75
Total Oxides	99.31	99.41	100.60
Ni	1.29	1.37	0.99
Co	0.073	0.061	0.070

3.2. Effect of mineralogy on the ores dissolution

The dissolution evidence of minerals contained in the ores during acid leaching can be observed by comparing the change in peak characteristics shown in XRD patterns between original ore samples and solid residues. Fig. 5 displays the XRD patterns of the original ore samples and their respective solid residues after leaching with HCl, HNO_3, and H_2SO_4. It is seen that the goethite peak with the reflection intensity at 21.3° 2θ (d_{101}=4.17 Å) in Ore-1 (Fig. 5A) remains appear after leaching with H_2SO_4 and HNO_3. However, its peak has been lost after leaching with HCl, indicating that goethite has been dissolved with this acid. The dissolution of lizardite, which was detected in the Ore-2 (Fig. 5B), shows a different response. Lizardite with a diagnostic peak at 12.16° 2θ (d_{001}=7.27 Å) has completely dissolved after leaching with H_2SO_4, but it has only partially dissolved in HCl and HNO_3. Similarly, gibbsite with a characteristic peak at 18.28° 2θ (d_{002}=4.84 Å) indicates less dissolution in H_2SO_4 and HNO_3, but it is strongly dissolved in HCl (Fig. 5C). Talc with a diagnostic peak at 9.50°2θ (d_{001}=9.32 Å) in all samples shows stronger intensity after leaching with H_2SO_4, implying that it was difficult to dissolve in H_2SO_4. On the contrary, the reflection of talc was diminished after leaching with HNO_3 and HCl, indicating that it is easily leached within these acids. Hematite exhibits relatively similar leaching behaviour with other phases such as lizardite and gibbsite; however, quartz with a diagnostic peak occurring at 26.63°

2θ (d_{011}=3.34 Å) relatively did not collapse, indicating that quartz was difficult to dissolve in all used acid solutions.

The proof of mineral dissolution during leaching with acid can also be observed by comparing the original texture and morphology of the limonite ores with the leached residues. Fig. 6 demonstrates the SEM images of original ore vs solid residue after leaching with 4 M HCl. As seen in Fig. 6A, the morphology of raw ore shows aggregate-like particles and porous, rough, and bumpy surfaces. In contrast, the morphology of solid residue, as shown in Fig. 6B, display smooth on the surface material and the particles have been undergoing shrinkage. In place, some line microcracks can also be observed.

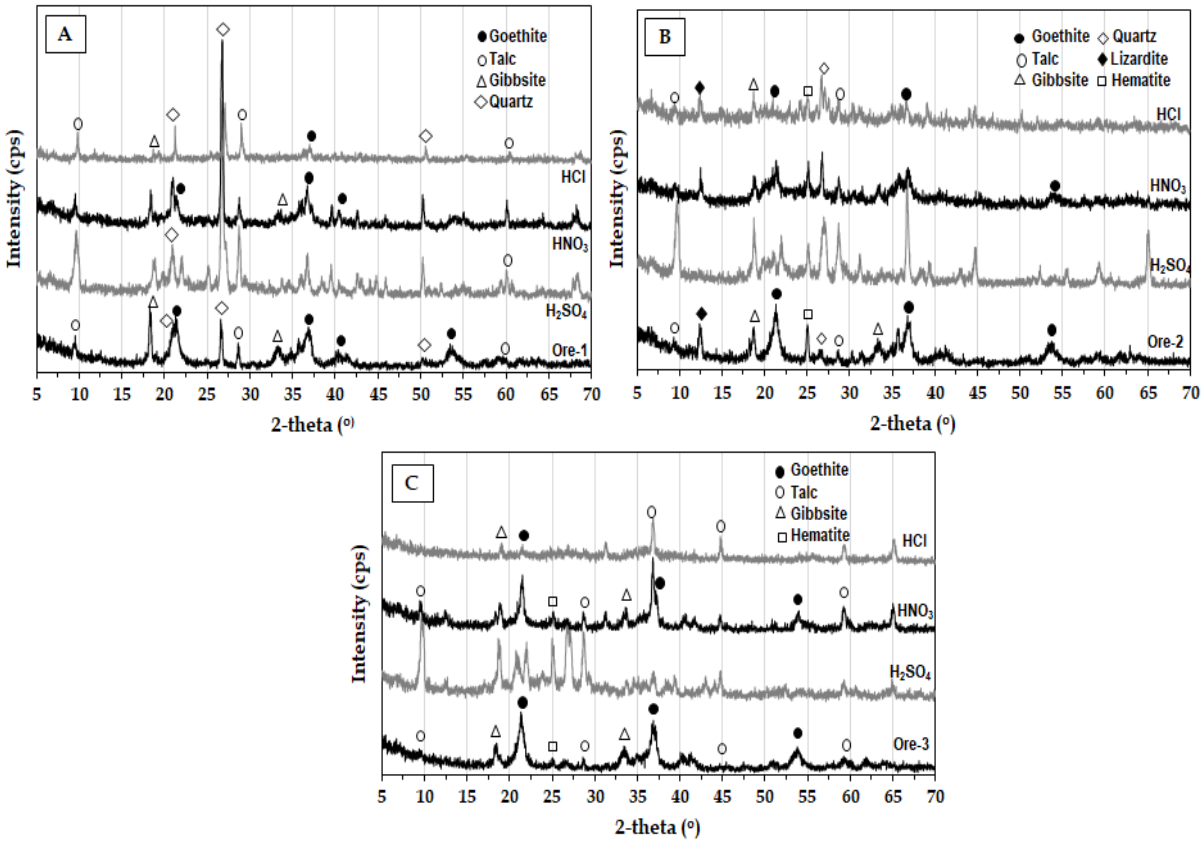

Fig. 5. Comparison of XRD patterns between original ores and solid residues leached using HCl, HNO_3 and H_2SO_4. Ore-1 (A), Ore-2 (B), and Ore-3 (C) from Lapaopao area after leaching at 100 °C with S/L of 1:7

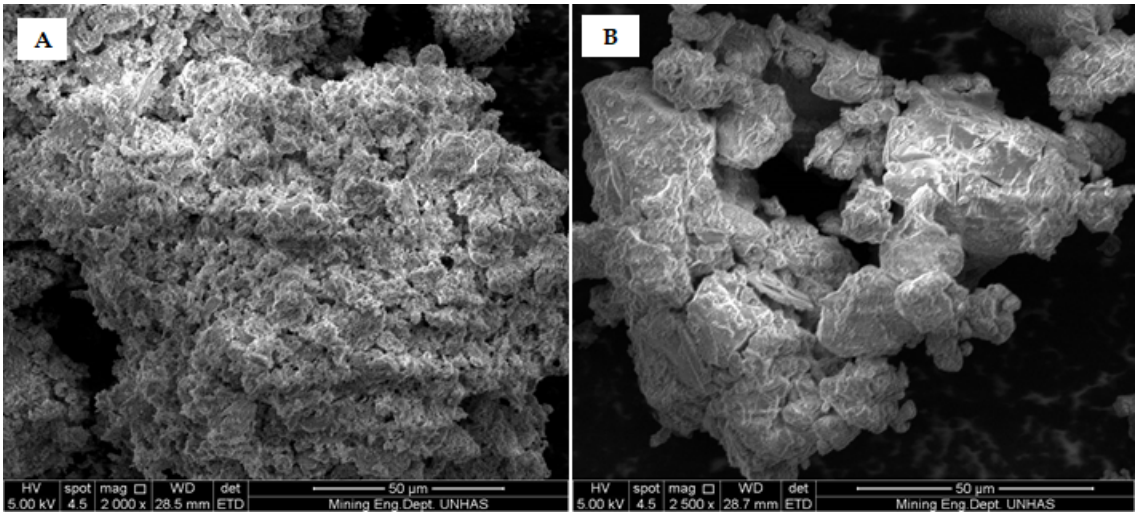

Fig. 6. SEM micrographs of original limonite Ore-1 (A) and leached residues (B) showing the changes of surface morphology after leaching with 4M HCl

Semi-quantitative analysis of leached residues was carried out on the basis of XRD data in order to calculate the mineral dissolution (φ_i) with the following equation (Eq.1)

$$\varphi_i = \left(1 - \frac{((w_{ri} \text{ x } mw_i)/\sum_i^n (w_{ri} \text{ x } mw_i)) \text{ x } m_r}{((w_{oi} \text{ x } mw_i)/\sum_i^n (w_{oi} \text{ x } mw_i)) \text{ x } m_o}\right) \text{ x } 100 \quad (1)$$

where: φ_i = dissolution rate of minerals, m_o = mass of ore, m_r = mass of residue, w_{oi} = % semi quantitative mineral i^{th} of ore, w_{ri} = % semi quantitative mineral i^{th} of residue, m_{wi} = mass of molecule of mineral i^{th}.

The dissolution degree of minerals in various ore types under HCl solution is shown in Table 3. It was indicated that the highest of mineral dissolution minerals was observed in the goethite which followed by gibbsite, lizardite and talc. With respect to thee individual ore minerals, goethite was the highest dissolution rate for the all ore samples, and the order of dissolution of goethite was found to be Ore-1>Ore-2>Ore-3. Gibbsite has higher dissolution rate in Ore-2, followed by Ore-1 and Ore 3. In contrast, talc more dissolved in Ore-3 as compared to Ore-1 and Ore-2. In the case of Ore-3, both goethite and gibbsite show the slow dissolution rates as compared to Ore-1 and Ore-2. This is likely the Ore-3 is dominated by talc where more acids were consumed to dissolve talc so that the chance of dissolution of goethite and gibbsite is lower in Ore-3 compared to Ore-1 and Ore-2. The rate of mineral dissolution is considerd caused by variations in the composition of Ni-bearing minerals, for example Lizardite which is quite abundant in Ore-2 so the dissolution level is higher than in Ore-1.

In addition, the dissolution behaviour of mineral using the three different inorganic acids was tested for Ore-2. The result of calculation of mineral dissolution rates are depicted in Table 4. It was demonstrated that goethite, as the mian Ni-bearing phase, has highest dissolution rate in HCl followed by in HNO_3 and in H_2SO_4. Similarly, gibbsite and talc have also higher dissolution rate in HCl. Whereas lizardite and hematite show higher dissolution rate in HNO_3. Despite quartz indicated lowest dissolution degree among the minerals containing in the ores, however, it also relatively dissolved with HNO_3. As shown in Table 4, it can be interpreted that the dissolution rates of minerals in ores treated by various acids show slightly different. Goethite, gibbsite and talc are found to have rapid dissolution in HCl followed by HNO_3 and then H_2SO_4. Meanwhile, for lizardite and hematite, it was revealed that fast mineral dissolution occurs in HCl then H_2SO_4 and HNO_3.

Table 3. Semi quantitative XRD analysis of minerals containing in the leach residues using HCL and the calculated of mineral dissolution of the three different ore samples

Mineral	Molar Mass	Leach Residue Mineralogy (%)			Dissolution of Mineral (%)		
		Ore-1	Ore-2	Ore-3	Ore-1	Ore-2	Ore-3
Goethite [FeO(OH)]	88.85	8.1	17.5	19.0	97.85	94.02	92.47
Gibbsite [$Al(OH)_3$]	77.94	31.9	4.5	27.0	82.05	95.27	80.51
Talc [$Mg_3(Si_4O_{10})(OH)_2$]	379.29	19.9	24.8	38.8	71.45	61.68	78.16
Lizardite [$Mg_3(Si_2O_5)(OH)_4$]	277.13	5.8	37.2	nd	68.00	86.14	nd
Hematite [a-Fe_2O_3]	159.69	nd*	nd	7.3	nd	100.00	92.81
Maghemite [g-Fe_2O_3]	159.69	0.8	nd	Nd	89.57	nd	nd
Quartz [SiO_2]	60.08	33.5	15.9	7.9	29.33	69.85	52.00
For mass balance							
Ore Wt (g)		37.50	37.50	37.50			
Residue Wt (g)		6.57	6.06	6.42			

*nd=not detected

3.3. Effect of acid types on the extraction of Ni and Co

The extraction of Ni and Co from the ores can be calculated by using the simple equation (Eq.2) with the following formula (Rao et al., 2023):

$$\chi = \frac{c \, x \, V}{mo \, x \, w} \text{ x } 100\% \quad (2)$$

where χ (%) is the extraction of metals; c (mg/L) and v (L) are the metal concentration and volume of PLS, respectively; m_o (g) and w (wt%/100) represent the mass of ore and metal content in the ore.

Fig. 7 illustrates the extraction of Ni and Co from three different limonite ores under the three types of inorganic acids. As shown in Fig. 7A, the extraction rate of Ni vs ore samples and acid types are different. However, the patterns of extraction rate of Ni from the ores in the three types of acids are similar in which HCl is highest leaching rate followed by HNO_3 and then H_2SO_4. A maximum 87% Ni could be extracted from Ore-1 under HCl solution, whereas only 85% and 70% of Ni could be obtained from the same sample using HNO_3 and H_2SO_4, respectively. Leaching of Ore-2 show slightly decreasing in all acid used and it is followed by Ore-3 leaching. Overall, the extraction of Ni in decreasing order are HCl>HNO_3>H_2SO_4.

Table 4 Semi quantitative XRD analysis of minerals containing in the Ore-2 leach residues and calculated mineral dissolution from the various acid treatment

Mineral	Molar Mass	Leach Residue Mineralogy (%)			Dissolution of Mineral (%)		
		HCl	HNO_3	H_2SO_4	HCl	HNO_3	H_2SO_4
Goethite [FeO(OH)]	88.85	17.5	12.9	15.4	94.02	91.34	88.43
Gibbsite [$Al(OH)_3$]	77.94	4.5	16.8	20.0	95.27	65.30	53.79
Talc [$Mg_3(Si_4O_{10})(OH)_2$]	379.29	24.8	28.3	29.4	61.68	14.11	0.19
Lizardite [$Mg_3(Si_2O_5)(OH)_4$]	277.13	37.2	30.5	18.3	86.14	77.69	85.02
Hematite [α-Fe_2O_3]	159.69	nd	4.0	0.7	100.00	70.20	94.17
Maghemite [-Fe_2O_3]	159.69	nd*	nd	nd	nd	nd	nd
Quartz [SiO_2]	60.08	15.9	7.4	16.2	69.85	72.44	32.51
For mass balance							
Ore Wt (g)		37.50	37.50	37.50			
Residue Wt (g)		6.06	11.98	11.93			

*nd=not detected

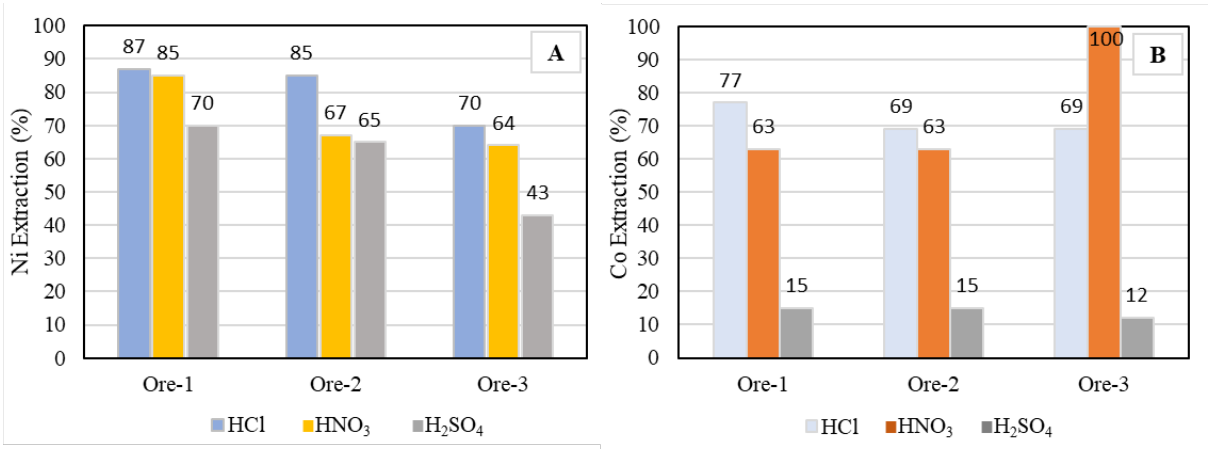

Fig. 7. Graphs showing the extraction of Ni (A) and Co (B) after atmospheric leaching of three different limonite ore samples from Lapaopao area (leaching at 100°C; S/L ratio 1:7; under HCl, HNO_3 and H_2SO_4 acid solutions).

In the case of Co extration (Fig. 7B), leaching behavior of Co from the Ore-1 and Ore-2 using three different acids looks similar. However, Co leaching from Ore-3 shows the opposite trend with Ni in terms of ore samples. A maximum of 100% Co could be extracted from Ore-3 using HNO_3. Extraction of Co using H_2SO_4 shows minimum values of 15% and 12% from the three ore samples. The extraction of Co using HCl show highest rate in Ore-1 reaching up to 77%. The higher leaching rate of Co in Ore-

3 using HNO_3 reveal that it is likely associated with Mn-mineral instead of goethite. It is confirmed by the higher concentration of Mn in Ore-3.

3.4. Leaching process of limonite ores in acids

The leaching mechanism of Ni and Co from limonite ore begins with a chemical reaction between acid and minerals containing in the ore, leading to breakdown of the crystal structure as a result of acid attack. During leaching process, nickel which is mainly hosted in the crystal lattices of goethite and lizardite, are expected to release into solution. The possible chemical reactions that occur during hydrochloric acid leaching of goethite and serpentine in limonite ore can be formulated as follows (Garces-Granda et al, 2020):

$$FeOOH_{(s)} + 3HCl_{(aq)} \rightarrow FeCl_{3(aq)} + 2H_2O_{(l)} \quad (3)$$

$$Mg_3Si_2O_5(OH)_{4(s)} + HCl(aq) \rightarrow 3MgCl_{2(aq)} + 2SiO_{2(s)} + H_2O_{(l)} \quad (4)$$

$$NiO_{(s)} + 2HCl_{(aq)} \rightarrow NiCl_{2(aq)} + H_2O_{(l)} \quad (5)$$

Dissolution of goethite, lizardite, and nickel oxide in nitric acid might take place through the following chemical reactions (Fathoni and Mubarok, 2015):

$$FeOOH_{(s)} + 3HNO_{3(aq)} \rightarrow Fe(NO_3)_{3(aq)} + 2H_2O_{(l)} \quad (6)$$

$$Mg_3Si_2O_5(OH)_4 + HNO_3 \rightarrow Mg(NO_3)_2 + 2SiO_2 + H_2O \quad (7)$$

$$NiO(s) + 2HNO_3(aq) \rightarrow Ni(NO_3)_2(aq) + H_2O(l) \quad (8)$$

Furthermore, dissolution of goethite and lizardite in sulfuric acid may follow the chemical reaction as shown below:

$$FeOOH(s) + H_2SO_4(aq) \rightarrow Fe(SO_4)_2(aq) + 2H_2O(l) \quad (8)$$

$$Mg_3Si_2O_5(OH)_4 + H_2SO_4 \rightarrow 3Mg(SO_4) + 2SiO_2 + H_2O \quad (9)$$

$$NiO(s) + 2H_2SO_4(aq) \rightarrow Ni(SO_4)_2(aq) + 2H_2O(l) \quad (10)$$

Based on XRD data of leached residues, it was generally indicated that the mineral dissolution rates in decreasing order were interpreted as follows: goethite > lizardite > gibbsite> hematite > talc> quartz. The extraction of Ni and Co from Ore-2 should be higher than that of Ore-1 because Ore-2 contains significant amounts of lizardite as a Ni bearing phase. However, in reality, the extraction rate of Ni from Ore-2 was lower than that of Ore-1 (Fig. 7A). This evidence could be due to the most of Ni-bearing phases in Ore-1 have been strongly dissolved, whereas Ni-bearing minerals in Ore-2, especially lizardite, might only partially leached out, called incongruent dissolution (Lacinska et al., 2016).

In the case of Ore-3, the lower Ni extraction might be due to the low content of Ni-bearing minerals (goethite and gibbsite, with 57% in total, see Table 1). It contains talc and hematite, more than 40% in total. Fortunately, talc, hematite, and quartz, having low dissolution rates in acid, are not expected to host Ni in their structures (Mcdonald and Whittington, 2008a). The low leaching rates of Ni in the Ore-3 as compared to the Ore-1 and Ore-2 could be deduced as follows: (i) the Ore-3 contains higher amounts of Ni-poor minerals such as gibbsite, talc, and hematite; (ii) goethite in Ore-3, as the main Ni-bearing phase, might contain appreciable amounts of substituted elements such as Cr and Al. These elements may humper the dissolution rate due to the higher bond strength of the M^{3+} - OH/O as compared to the Fe^{3+}-OH/O (Ugwu and Sherman, 2019). The comparison of surface morphologies between ore and solid residue particles (Fig. 6) shows that ore dissolution mechanism follows a shrinking core particle model (Levenspiel, 1999; Didyk-Mucha et al., 2016). Reactions are assumed to occur first on the outer surface of ore particles. The porous areas infiltrate into solid particles, where the particles experience shrinkage during the leaching process. Three subprocesses may take place during leaching: (i) external diffusion of acid on the particle surface; (ii) inward diffusion of solution on the porous zones into the core surface; and (iii) leaching reaction on the inner core.

Another factor that might affect the dissolution rate of minerals in limonite ores is the reactivity of lixiviants. Hydrochloride acid is likely more reactive than sulfuric acid (McDonald and Whittington, 2008b). Despite H_2SO_4 having two protons, only one proton is readily released into solution, whereas another (second) proton is more difficult to liberate in solution, leading to incomplete dissociation (Laird, 2009). The reactivity of HCl is higher than that of HNO_3 because, during the leaching process,

protonation of HCl results in Cl ionization. The presence of Cl- in solution may accelerate mineral dissolution rate due to the formation of Fe-Cl complex on the surface minerals (Gardes-Granda et al., 2020). In contrast, the existence of NO_3^- through the complete dissociation of HNO_3 does not form any surface complex with Fe (He et a., 2022). Our study was in agreement with the dissolution kinetics of laterite reported by Ayanda et al. (2011), who found that HCl was most reactive, followed by HNO_3 and then H_2SO_4.

Conclusions

Leaching experiments of the three limonite ore samples from Lapaopao, Southeast Sulawesi, using three different acids (HCl, HNO_3, and H_2SO_4) have been conducted. Based on the results and discussions mentioned above, some conclusions can be drawn as follows:

1. The mineralogical composition of the studied ore samples is dominated by goethite, but gibbsite, lizardite, and talc are also present in significant amounts. Goethite is thought to be the most common Ni-host mineral in the studied ores. The highest concentration of Fe_2O_3 with very low Mg demonstrate that such ores are best classified as oxide ore or limonite.
2. The analysis results of solid residues indicate that the dissolution rates of limonite ores were found to decrease in the order of Ore-1 > Ore-2 > Ore-3. The dissolution mechanism follows the shrinking core model via a diffusion-controlled process.
3. The results of the leaching experiment demonstrate that HCl provided the highest extraction of Ni with a value of 87%, compared to HNO_3 with a value of 85% and H_2SO_4 with a value of 70%. This is in accordance with the higher reactivity of HCl combined with the formation of Fe-Cl complexes on the mineral surface, which may enhance the dissolution of minerals during the leaching process.

Acknowledgments

This research is financially supported by PT Ceria Nugraha Indotama (PT CNI). We would like to express our gratitude to PT CNI Management and Staff for their generous support during the research. Special thanks are directed to the Exploration Department staff, who have provided the assistance during our field work. A great thanks is due to the Head of Mining Engineering Department, Hasanuddin University for their great assistance in providing unlimited access to the facilities while conducting laboratory experiments until the completion of the work. We would also like to express our sincere thanks to the two anonymous reviewers whose suggestions helped improve the earlier version of this manuscript.

References

AGATZINI-LEONARDOU, S., TSAKIRIDIS, P.E., OUSTADAKIS, P., KARIDAKIS, T., KATSIAPI, A., 2009. *Hydrometallurgical process for the separation and recovery of nickel from sulphate heap leach liquor of nickeliferrous laterite ores*. Miner. Eng. 22, 1181–1192.

AYANDA, O.S., ADEKOLA, F.A., BABA, A.A., FATOKI, O.S., XIMBA, B.J., 2011. *Comparative Study of the Kinetics of Dissolution of Laterite in some Acidic Media*. J. Miner. Mater. Charact. Eng. 10, 1457–1472.

BUTT, C.R.M., 2007. *Nickel laterites: Characteristics, classification, and processing options*. In: Cooperative Research Centre For Landscape Environments and Mineral Exploration. Unpublished.

CARVALHO-E-SILVA, M.L., RAMOS, A.Y., NOGUEIRATOLENTINO, H.C., ENZWEILER, J., NETTO, S.M., ALVES, M. DO C.M., 2003. *Incorporation of Ni into natural goethite: An investigation by X-ray absorption spectroscopy*. Am. Mineral. 88, 876–882.

CORNELL, R.M., SCHWERTMANN, U., 2006. *The Iron Oxides: Structure, Properties, Reactions, Occurrences and Uses, 2nd, Completely Revised and Extended Edition, 2nd ed*. John Wiley & Sons, Inc, New York.

DALVI, A.D., BACON, W.G., OSBORNE, R.C., 2004. *The Past and the Future of Nickel Laterites*. PDAC 2004 Int. Conv. 1–27.

DIDYK-MUCHA, A., PAWLOWSKA, A., SADOWSKY, Z., 2016. *Application of the shrinking core model for dissolution of serpentinite in an acid solution,* E S Web of Conferences, 8, 01035

FATHONI, M.W., and MUBAROK, M.Z., 2015. *Study on the Leaching Behavior of Limonite Nickel Ore from Halmahera Island in Nitric Acid Solution,* Majalah Metalurgi. 30, 115 – 124.

GARCES-GRANDA, A., LAPIDUS, G.T., AND RESTREPO-BAENA, O.J. 2020. *Effect of a thermal pretreatment on dissolution kinetics of a limonitic laterite ore in chloride media.* Hydrometallurgy. 196, 105438.

GHARAEI, A.A., REZAI, B., SHOORMASTI, H.H., 2019. *X-Ray mapping and the mineralogy pattern of nickel laterite ore*: Bavanat, Fars, Iran 10, 811–820.

GOLIGHTLY, J.P., 1979. *Nickeliferous laterites: A general description, in Evans*, D.J.I., Shoemaker, R.S. and Veltman, H., eds. Int. Laterite Symp. New York, Soc. Min. Eng. 3–23.

HE, F., MA, B., WANG, C., CHEN, Y. 2022. *Mineral evolution and porous kinetics of nitric acid pressure leaching limonitic laterite*. Miner. Eng. 181, 107544.

INTERNATIONAL ENERGY AGENCY (IEA), 2022. *Global EV Outlook 2022 - Securing supplies for an electric future*. Glob. EV Outlook 2022 221.

INTERNATIONAL NICKEL STUDY GROUP, 2021. *The world nickel factbook 2021*.

KYLE, J., 2010. *Nickel laterite processing technologies – where to next?,* in: ALTA 2010 Nickel/Cobalt/Copper Conference. ALTA Metallurgical Services Publications, Melbourne, Australia, 1–39.

LACINSKA, A.M., STYLES, M.T., BATEMAN, K., WAGNER, D., HALL, M. R., GOWING, C., BROWN, P.D., 2016. *Acid-dissolution of antigorite, chrysotile and lizardite for ex situ carbon capture and storage by mineralization*, Chem. Geol. 437, 153 – 169.

LAIRD, B.B., 2009. *University Chemistry*, The McGraw-Hill Companies, Inc. New York, 893 p.

LEVENSPIEL, O., 1999. *Chemical Reaction Engineering* (3rd Ed), John Wiley & Sons, New York,

MARSH, E., ANDERSON, E., GRAY, F., 2013. *Mineral Deposit Models for Resource Assessment.* In: Nickel-Cobalt Laterites—A Deposit Model. U.S. Geological Survey Scientific Investigations Report 2010–5070–H, p. 38.

MCDONALD, R.G., & WHITTINGTON, B.I., 2008a. *Atmospheric acid leaching of nickel laterites review. Part I. Sulphuric acid technologies*. Hydrometallurgy, 91, 35–55.

MCDONALD, R.G., & WHITTINGTON, B.I., 2008b. *Atmospheric acid leaching of nickel laterites review. Part II. Chloride and bio-technologies.* Hydrometallurgy 91, 56–69.

ÖNAL, M.A.R., & TOPKAYA, Y.A., 2014. *Pressure acid leaching of Çaldağ lateritic nickel ore: An alternative to heap leaching*. Hydrometallurgy.

PARAWANGSA, A., PRATOMO, H., HEHANUSA, R., 2021. *Exporation Report PT Ceria Nugraha Infotama 2021*, Unpublished.

PELLETIER, B., 1996. *Serpentines in nickel silicate ores from New Caledonia,* in Grimsey, E.J., and Neuss, I. (eds). Nickel '96. Australas. Inst. Min. Metall. Melb. 6, 197–205.

PUTZOLU, F., BALASSONE, G., BONI, M., MACZURAD, M., MONDILLO, N., NAJORKA, J., PIRAJNO, F., 2018. *Mineralogical association and Ni-Co deportment in the Wingellina oxide-type laterite deposit (Western Australia)*. Ore Geol. Rev. 97, 21–34.

RAO, M., CHEN, J., ZHANG, T., HU, M., YOU, J., LUO, J., 2023. *Atmospheric acid leaching of powdery Ni-Co-Fe alloy derived from reductive roasting of limonitic laterite ore and recovery of battery grade iron phosphate.* Hydrometallurgy. 218, 106058.

STANKOVIĆ, S., STOPIĆ, S., SOKIĆ, M., MARKOVIĆ, B., FRIEDRICH, B., 2020. *Review of the past, present, and future of the hydrometallurgical production of nickel and cobalt from lateritic ores*. Metall. Mater. Eng. 26, 199 – 208.

TEITLER, Y., FAVIER, S., AMBROSI, J. P., SEVIN, B., GOLFIER, F., & CATHELINEAU, M. 2022. *Evaluation of Sc concentrations in Ni-Co laterites using Al as a geochemical proxy*. *Minerals*, *12*(5), 615.

UGWU, I. M. and SHERMAN, D. M., 2019. *The solubility of goethite with structurally incorporated nickel and cobalt: Implication for laterites*. Chemical Geology, 518, 1 – 8.

TOP, S., KURSUNOGLU, S., ICHLAS, Z.T., 2020. *Effects of leaching parameters on the dissolution of nickel, cobalt, manganese and iron from Caldag lateritic nickel ore in hydrochloric acid solution*. Can. Metall. Quart. 59, 368–376.

WANG, B., GUO, Q., WEI, G., ZHANG, P., QU, J., QI, T., 2012. *Characterization and atmospheric hydrochloric acid leaching of a limonitic laterite from Indonesia*. Hydrometallurgy 129–130, 7–13.

WHITNEY, D.L., EVANS, B.W., 2010. *Abbreviations for names of rock-forming minerals*. Am. Mineral. 95, 185–187.

WHITWORTH, A. J., VAUGHAN, J., SOUTHAM, G., VAN DER ENT, A., NKRUMAH, P. N., MA, X., & PARBHAKAR-FOX, A. 2022. *Review on metal extraction technologies suitable for critical metal recovery from mining and processing wastes*. Minerals Engineering, 182, 107537.